Am J Physiol Heart Circ Physiol 282: H1018–H1034, 2002.
First published November 8, 2001; 10.1152/ajpheart.00231.2001.

Theoretical analysis of rest and exercise hemodynamics in patients with total cavopulmonary connection

ELISA MAGOSSO, SILVIO CAVALCANTI, AND MAURO URSINO
Department of Electronics, Computer Science and Systems, University of Bologna, 40136 Bologna, Italy

Received 23 March 2001; accepted in final form 5 November 2001

Magosso, Elisa, Silvio Cavalcanti, and Mauro Ursino. Theoretical analysis of rest and exercise hemodynamics in patients with total cavopulmonary connection. *Am J Physiol Heart Circ Physiol* 282: H1018–H1034, 2002. First published November 8, 2001; 10.1152/ajpheart.00231.2001.—The objective of this study was to determine the impact of a total cavopulmonary connection on the main hemodynamic quantities, both at rest and during exercise, when compared with normal biventricular circulation. The analysis was performed by means of a mathematical model of the cardiovascular system. The model incorporates the main parameters of systemic and pulmonary circulation, the pulsating heart, and the action of arterial and cardiopulmonary baroreflex mechanisms. Furthermore, the effect of changes in intrathoracic pressure on venous return is also incorporated. Finally, the response to moderate dynamic exercise is simulated, including the effect of a central command, local metabolic vasodilation, and the "muscle pump" mechanism. Simulations of resting conditions indicate that the action of baroreflex regulatory mechanisms alone can only partially compensate for the absence of the right heart. Cardiac output and mean systemic arterial pressure at rest show a large decrease compared with the normal subject. More acceptable hemodynamic quantity values are obtained by combining the action of regulatory mechanisms with a chronic change in parameters affecting mean filling pressure. With such changes assumed, simulations of the response to moderate exercise show that univentricular circulation exhibits a poor capacity to increase cardiac output and to sustain aerobic metabolism, especially when the oxygen consumption rate is increased above 1.2–1.3 l/min. The model ascribes the poor response to exercise in these patients to the incapacity to sustain venous return caused by the high resistance to venous return and/or to exhaustion of volume compensation reserve.

Fontan procedure; computer modeling; cardiovascular regulation; baroreflex

COMPLEX FORMS of congenital heart disease may impose surgical reconstructive procedures, creating new cardiovascular anatomy and hemodynamics. The most striking examples are right heart-bypass operations (generally termed Fontan's operations) used in a variety of congenital cardiac malformations such as tricuspid atresia, right ventricle hypoplasia, and pulmonary atresia (6, 7, 10, 27, 35). In these patients, only the left side of the heart pumps blood properly. One such operation consists in a total cavopulmonary connection, whereby the systemic venous blood in the inferior and superior vena cava is rerouted directly to the pulmonary arteries without the benefit of the normal right ventricle. In this situation the pulmonary and systemic circulation are in series with only one pumping chamber.

Generally, patients who have undergone Fontan's procedure have a good prognosis, although they have subnormal cardiac output (CO) at rest (36, 42) while central venous pressure is significantly elevated (15, 22). Nevertheless, many studies report an attenuated CO response to exercise in Fontan's subjects, even in asymptomatic patients (2, 36, 42). The abnormal cardiac response to exercise is attributed to cardiac factors, such as the absence of right ventricle function, defective sinus node rhythm, and impaired left ventricular function. However, because of the mechanical coupling between heart and peripheral circulation, inadequate CO response to exercise might also depend on insufficient peripheral vascular adjustments. Unfortunately, only a few studies have investigated to what extent the exclusion of the pumping chamber between the systemic and pulmonary side may affect the entire circulation (15, 16, 34); in particular, the role of the autonomic regulatory mechanisms is unclear, especially in the compensatory response to exercise.

Accordingly, the present work was designed with two main purposes: *1*) to determine the influence of the main hemodynamic factors in the maintenance of univentricular circulation (UC) under resting conditions; and *2*) to test the hypothesis that during exercise, compensatory mechanisms are unable to maintain venous return in the UC, thus resulting in insufficient CO and a severe limitation of the maximal oxygen consumption rate. Hence, the abnormal state may be concealed at rest but could appear under stressful conditions, such as dynamic exercise, when the system, which has in part exhausted its resources, is greatly stimulated.

Addressing this issue directly in the univentricular patients is obviously limited by technical and ethical reasons. Moreover, in vivo it is almost impossible to examine the influence of a single parameter on the total circulation because of the complex interrelationships existing among pressure, flow, resistance, and

Address for reprint requests and other correspondence: E. Magosso, DEIS, Viale Risorgimento 2, 40136 Bologna, Italy (E-mail: emagosso@deis.unibo.it)

The costs of publication of this article were defrayed in part by the payment of page charges. The article must therefore be hereby marked "*advertisement*" in accordance with 18 U.S.C. Section 1734 solely to indicate this fact.

capacitance, further complicated by the action of reflex regulatory mechanisms. Mathematical cardiovascular system models and computer simulations may represent a valid support for the analysis of this problem. A computer model, in fact, allows the hemodynamic effects of individual parameter changes to be investigated in rigorously quantitative terms.

To answer the abovementioned points, in this study we improved a mathematical model of the cardiovascular system, including baroreflex control under pulsating conditions (40). Hemodynamic data, reproduced by this model with both left and right pumps, are considered as the reference for functioning circulation. The model was then modified through a direct connection of systemic and pulmonary circulation bypassing the right heart. This modified model has been used to study which compensatory mechanisms are effective in maintaining UC both at rest and during exercise.

Glossary

A	Peak value of intramuscular pressure, mmHg
AP	Arterial pressure, mmHg
B_θ	Offset term to simulate a chronic alteration in the corresponding effector response, spikes/s
CO	Cardiac output, ml/s
C_j (j = ep, mp)	Extrasplanchnic and skeletal muscle peripheral compliance, respectively, ml/mmHg
C_j (j = ev, sv, mv, v)	Extrasplanchnic, splanchnic, muscle, and systemic thoracic venous compliance, respectively, ml/mmHg
$E_{max,lv}$	Left ventricular end-systolic elastance (i.e., the slope of the left ventricular end-systolic pressure-volume curve), mmHg/ml
$E_{max,rv}$	Right ventricular end-systolic elastance (i.e., the slope of the right ventricular end-systolic pressure-volume curve), mmHg/ml
f_{ab}	Afferent activity from arterial baroreceptors, spikes/s
f_{ac}	Afferent activity from cardiopulmonary baroreceptors, spikes/s
$f_{es,j}$ (j = p, v, h)	Discharge frequency in efferent sympathetic fibers to arterioles, veins, and the heart, respectively, spikes/s
$f_{es,min}$	Minimum sympathetic stimulation, spikes/s
f_{ev}	Efferent vagal discharge frequency, spikes/s
$f_{max,l}$	Upper saturation of discharge frequency at cardiopulmonary baroreceptors, spikes/s
$f_{es,cc}$, $f_{ev,cc}$	Offset term in the efferent sympathetic responses and in the efferent vagal response, respectively, reproducing the effect of motor central command on cardiovascular control centers, spikes/s
F_e	Total extrasplanchnic flow (i.e., flow through the parallel of R_{ep} and R_{mp}), ml/s
$F_{o,m}$	Blood flow leaving leg muscle veins (i.e., blood flow through R_{mv}), ml/s
$G_{ab,j}$ (j = p, v, h)	Constant gain linking afferent activity from arterial baroreceptors to efferent sympathetic activity directed to peripheral arterioles, veins, and heart, respectively, dimensionless
$G_{ab,vag}$	Constant gain linking afferent activity from arterial baroreceptors to vagal efferent activity, dimensionless
$G_{ac,j}$ (j = p, v, h)	constant gain linking afferent activity from cardiopulmonary baroreceptors to efferent sympathetic activity directed to peripheral arterioles, veins, and heart, respectively, dimensionless
$G_{ac,vag}$	Constant gain linking afferent activity from cardiopulmonary baroreceptors to vagal efferent activity, dimensionless
G_d	Active muscle conductance, ml/(s·mmHg)
G_l	Gain at the central point of the cardiopulmonary, baroreceptor response, spikes/(s·mmHg)
G_θ	Strength of the corresponding effector mechanism, (effector dimension)·s
HR	Heart rate, beats/min
k_l	Parameter related to the central gain of cardiopulmonary baroreceptor response, mmHg
LBNP	Lower body negative pressure, mmHg
MAP	Mean arterial pressure, mmHg
NC	Normal (biventricular) circulation

P_0	Constant parameter in the pressure-volume relationship of active muscle veins, with the dimension of pressure, mmHg
P_l	Output variable of the low-pass filter, mmHg
P_{im}	Intramuscular pressure (i.e., extravascular pressure at active muscle veins), mmHg
P_{la}	Pressure inside left atrium, mmHg
P_{sa}	Systemic arterial pressure, mmHg
P_{pa}	Pressure inside pulmonary arteries, mmHg
P_{pv}	Pressure inside pulmonary veins, mmHg
P_{mcf}	Mean circulatory filling pressure, mmHg
P_{mv}	Pressure inside leg skeletal muscle veins, mmHg
P_{thor}	Intrathoracic pressure (i.e., extravascular pressure at vessels located inside the thoracic cavity), mmHg
$P_{thor,max}$	Intrathoracic pressure at the end of expiration, mmHg
$P_{thor,min}$	Intrathoracic pressure at the end of inspiration, mmHg
P_{tn}	Pulmonary venous transmural pressure at the central point of the static sigmoidal characteristic of cardiopulmonary baroreceptors, mmHg
P_v	Pressure inside systemic thoracic veins, mmHg
R_d (= $1/G_d$)	Resistance arranged in parallel to R_{mp} to simulate muscle vasodilation during exercise, mmHg·s·ml^{-1}
R'_{ep}	Total extrasplanchnic resistance (i.e., the parallel of R_{ep} and R_{mp}), mmHg·s·ml^{-1}
R_j (j = ev, mv, v)	Extrasplanchnic, leg skeletal muscle, and thoracic venous resistance, respectively, mmHg·s·ml^{-1}
R_j (j = pa, pp, pv)	Pulmonary artery, pulmonary peripheral, and pulmonary venous resistance, respectively, mmHg·s·ml^{-1}
R_j (j = ep, sp, mp)	Extrasplanchnic, splanchnic, and leg skeletal muscle peripheral resistance, respectively, mmHg·s·ml^{-1}
$s(t)$	Dimensionless variable ranging between 0 and 1, which represents the fraction of the respiratory cycle
T	Heart period, s
T_c	Duration of the muscular contraction, s
T_e	Expiration time, s
T_i	Inspiration time, s
T_{im}	Overall duration of the muscular contraction-relaxation cycle, s
T_{resp}	Respiratory period, s
UC	Univentricular circulation
$\dot{V}_{O_2}$	Oxygen consumption rate, l/min
$\dot{V}_{O_2\,max}$	Upper bound for oxygen consumption rate, l/min
$V'_{u,ev}$	Total extrasplanchnic venous unstressed volume (i.e., $V_{u,ev} + V_{u,mv}$), ml
$V_{u,lv}$	x-Axis intercept of the left ventricular end-systolic pressure-volume curve, ml
$V_{u,j}$ (j = ep, mp)	Unstressed volume in extrasplanchnic and leg skeletal muscle peripheral circulation, respectively, ml
$V_{u,j}$ (j = ev, sv, mv)	Extrasplanchnic, splanchnic, and skeletal muscle venous unstressed volume, respectively, ml
V_{mv}	Total blood volume in leg skeletal muscle, ml
V_t	Total amount of blood contained in cardiovascular system, ml
τ_l	Time constant of the cardiopulmonary baroreceptor response, s
θ_0	Value of the effector in the absence of any sympathetic drive, effector dimension
θ	Generic effector: peripheral resistances (mmHg·s·ml^{-1}); venous unstressed volumes (ml); heart contractility (mmHg/ml)
ϵ	State variable used to define $s(t)$; i.e., $s(t)$ = frac[$\epsilon(t)$], dimensionless
$\psi(t)$	Activation function of skeletal muscle fibers, dimensionless
$\alpha(t)$	Dimensionless variable ranging between 0 and 1, which represents the fraction of the muscular contraction-relaxation cycle
$\zeta(t)$	State variable used to define $\alpha(t)$; i.e., $\alpha(t)$= frac [$\zeta(t)$], dimensionless

QUALITATIVE MODEL DESCRIPTION

Hemodynamics in a normal subject, at rest and in response to a stress condition, were simulated using the mathematical model presented by Ursino (40), to which a few improvements were made. The improvements concern the following points. The first point concerns the inclusion of the mechanical effects of respiration on the cardiovascular system occurring through variations in intrathoracic pressure (see APPENDIX). Inclusion of the negative intrathoracic pressure in the model is important because respiratory factors may contribute to drive the blood flow into the lungs, especially in patients with UC. The second point concerns the inclusion of cardiopulmonary baroreceptors. The latter, in fact, may be particularly important in cardiovascular regulation, especially under the hemodynamic conditions (characterized by a reduced pulmonary venous pressure) typical of UC. The third point is the subdivision of the systemic circulation into three distinct parallel branches. These represent the splanchnic circulation, circulation in the skeletal muscle of legs, and circulation in the remaining extrasplanchnic vascular beds. Separation of the vascular bed of the skeletal muscle of legs from the others is important to simulate dynamical exercise of the lower limbs (see below). The final point is a description of the main cardiovascular adjustments (both reflex and local) that occur during moderate dynamic exercise.

The model for the univentricular patient has been developed starting from the one valid for the normal subject, bypassing the right heart. An accurate model description for a normal subject, including equations and parameter assignment, may be found in a previous paper (40). In the APPENDIX, only the mathematical equations describing the new aspects of the model are reported. All new parameter values are listed in Table 1. In the following, the main characteristics of the models are presented in qualitative terms, stressing new features in particular.

The cardiovascular system. The hydraulic analog of the circulatory system in the normal subject is shown in Fig. 1. The vascular system includes pulmonary and systemic circulation. The former consists of the serial arrangement of three compartments mimicking the arterial, peripheral, and venous pulmonary vascular beds (subscripts pa, pp, and pv, respectively). Systemic circulation is described by means of eight compartments. These include the large arteries (subscript sa), the peripheral and venous circulation in the splanchnic (subscripts sp and sv), leg skeletal muscle (subscripts mp and mv), and extrasplanchnic (subscripts ep and ev) vascular beds, and the systemic veins into the thorax (subscript v). The latter compartment, which was not included in the previous version, has been added to take into account the fact that veins traverse cavities with a different pressure ambient (25). Each compartment is akin to an elastic chamber that exchanges flow with the downstream and upstream compartments through hydraulic resistances. Blood volume in each compartment is expressed as the sum of two contributions: the unstressed volume (defined as the volume at null transmural pressure) and the stressed volume, which accounts for the elastic deformation due to vessel compliance. A more complex pressure-volume curve has been adopted for the veins in the active muscle at negative transmural pressure to describe the so-called "muscle pump" dur-

Table 1. *Parameter values*

Parameters Characterizing Vascular System Under Basal Conditions			
$R_{ep} = 1.725$ mmHg·s·ml^{-1}	$C_{ep} = 1.36$ ml/mmHg		$V_{u,ep} = 274.1$ ml
$R_{mp} = 7.423$ mmHg·s·ml^{-1}	$C_{mp} = 0.31$ ml/mmHg		$V_{u,mp} = 62.5$ ml
$R_{ev} = 0.0197$ mmHg·s·ml^{-1}	$C_{ev} = 28.4$ ml/mmHg		$V_{u,ev} = 1{,}120$ ml
$R_{mv} = 0.0848$ mmHg·s·ml^{-1}	$C_{mv} = 6.6$ ml/mmHg		$V_{u,mv} = 255$ ml
$P_0 = 3.9$ mmHg	$C_{sv} = 43.11$ ml/mmHg		
$R_v = 0.0054$ mmHg·s·ml^{-1}	$C_v = 33$ ml/mmHg		
Parameters Characterizing Cardiopulmonary Baroreceptors			
$f_{max,l} = 20$ spikes/s	$G_l = 3.5$ ν/s·mmHg	$P_{tn} = 10.8$ mmHg	
$G_{ac,p} = 2.5$	$G_{ac,v} = 0$	$G_{ac,h} = 2$	$G_{ac,vag} = -1$
Parameters of Cardiovascular Effectors			
$G_{R,ep} = 0.653$ mmHg·s·ml^{-1}·ν^{-1}	$R_{ep,0} = 0.96$ mmHg·s·ml^{-1}	$G_{Vu,ev} = -107.5$ ml/ν	$V_{u_{ev,0}} = 1{,}247$ ml
$G_{R,mp} = 2.81$ mmHg·s·ml^{-1}·ν^{-1}	$R_{mp,0} = 4.13$ mmHg·s·ml^{-1}	$G_{Vu,mv} = -25$ ml/ν	$V_{u_{mv,0}} = 290$ ml
Parameters of Intramuscular Pressure			
$A = 50$ mmHg	$T_{im} = 1$ s		$T_c = 0.75$ s

	Rest	Exercise ($\dot{V}O_2 = 1$ l/min)	Exercise ($\dot{V}O_2 = 2$ l/min)
Parameters of Intrathoracic Pressure			
$T_{resp} =$	4 s	3 s	2 s
$T_i =$	1.6 s	1.4 s	1 s
$T_e =$	1.4 s	1.6 s	1 s
$P_{thor,max} =$	−4 mmHg	−4 mmHg	−2 mmHg
$P_{thor,min} =$	−9 mmHg	−12 mmHg	−15 mmHg
Parameters Reproducing Central Command and Metabolic Muscle Vasodilation			
$f_{es,cc} =$	0 spikes/s	6.5 spikes/s	15 spikes/s
$f_{ev,cc} =$	0 spikes/s	1.8 spikes/s	3.5 spikes/s
$R_d =$	10^4 mmHg·s·ml^{-1}	0.9 mmHg·s·ml^{-1}	0.6 mmHg·s·ml^{-1}

See *Glossary* for definitions. ν = spikes/s.

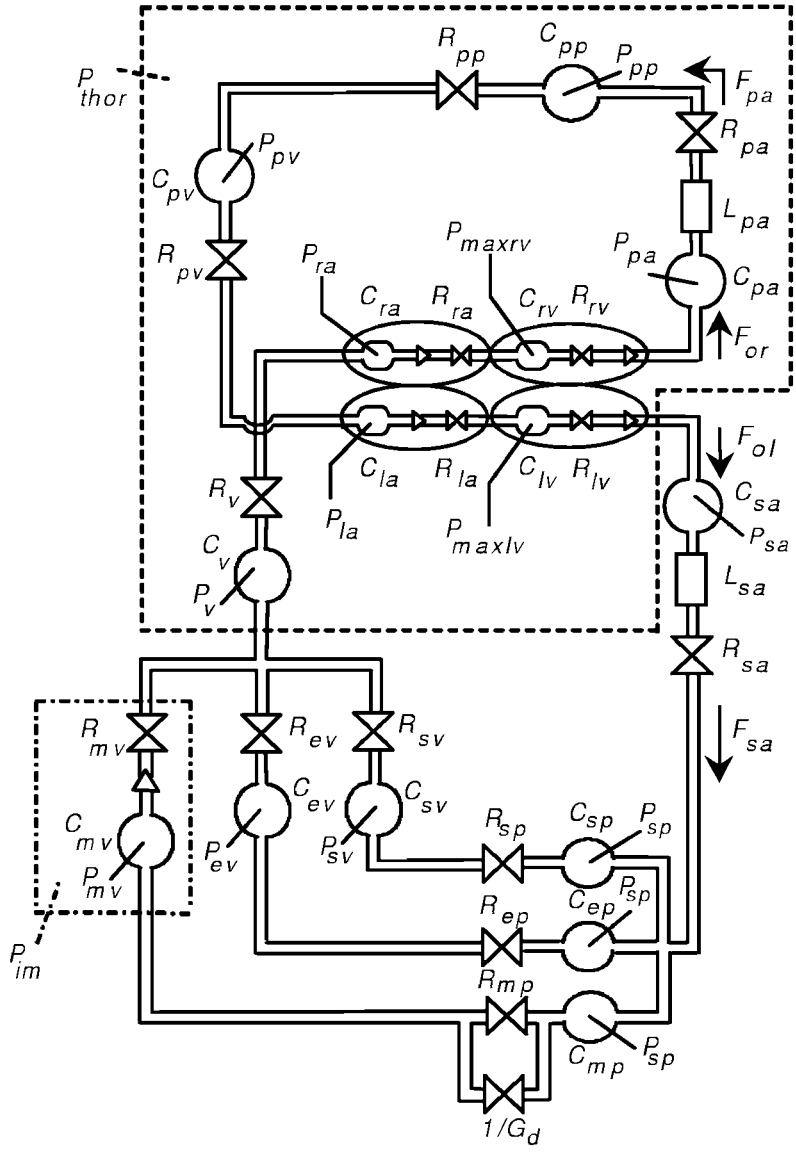

Fig. 1. Hydraulic analog of the cardiovascular system in the normal subject. P, pressures; *R*, hydraulic resistances; C, compliances; *L*, inertances; F, flows; sa, systemic arteries; sp and sv, splanchnic peripheral and splanchnic venous circulation; ep and ev, extrasplanchnic peripheral and extrasplanchnic venous circulation; mp and mv, peripheral and venous circulation in active muscle compartment; v, systemic thoracic veins; ra, right atrium; rv, right ventricle; pa, pulmonary arteries; pp and pv, pulmonary peripheral and pulmonary venous circulation; la, left atrium; lv, left ventricle. G_d, conductance used to simulate muscle vasodilation during exercise. Dashed line delimits the portion of cardiovascular system located inside the thoracic chamber; P_{thor}, intrathoracic pressure; P_{im}, intramuscular pressure; i.e., the extravascular pressure of active muscle veins (surrounded by a dash-dot line).

ing exercise (*Eq. A1* in the APPENDIX). Inertial effects have only been included in the large artery compartments (inertances L_{sa} and L_{pa}), where blood acceleration is significant.

The right and left sides of the heart (see Fig. 1) embody a passive atrium (described via a linear capacity) and a pulsating ventricle. The contractile activity of the ventricle is simulated by a time-varying elastance, reproducing the isometric pressure-volume curve in series with a time-varying resistance, which mainly reflects the viscosity of the ventricle. The shift from the end-diastolic to the end-systolic pressure-volume curve is governed by a periodic excitation, mimicking the sinus pacemaker.

To account for the respiratory effects on cardiovascular hemodynamics, the extravascular pressure has been given a different value in the portion located inside the thoracic cavity (i.e., heart, lungs, and thoracic veins, surrounded in Figs. 1 and 2 by a dashed line) and in the remaining vessels. The intrathoracic pressure changes periodically as a consequence of respiration (*Eqs. A3* and *A4* in the APPENDIX). According to experimental data (25), we assumed that intrathoracic pressure (P_{thor}) in the model falls linearly during inspiration (down to −9 mmHg) and then rises linearly during expiration to recover the steady value of the respiratory pause (approximately equal to −4 mmHg). Moreover, as will be described in *Response to moderate dynamic exercise*, the pattern of intrathoracic pressure varies (both as its duration and amplitude) during exercise. Furthermore, we assumed that the extravascular pressure outside the thoracic chamber remains constant at the same value as atmospheric pressure, with the exception of extravascular pressure in the active muscle, which varies rhythmically during dynamic exercise. These assumptions allow respiratory fluctuations in the main hemodynamic quantities (arterial blood pressure, venous return, left and right stroke volume) to be reproduced fairly well (13, 19).

To reproduce the right heart bypass (see Fig. 2), the pulmonary artery compartment has been directly coupled to the systemic veins. This arrangement mimics the conditions occurring after a total cavopulmonary operation. Under this condition the left ventricle faces the serial arrangement of the systemic and pulmonary resistances, i.e., the total vascular resistance. The effect of different surgical procedures might be simulated by suitably varying parameters R_v and C_v in Fig. 2.

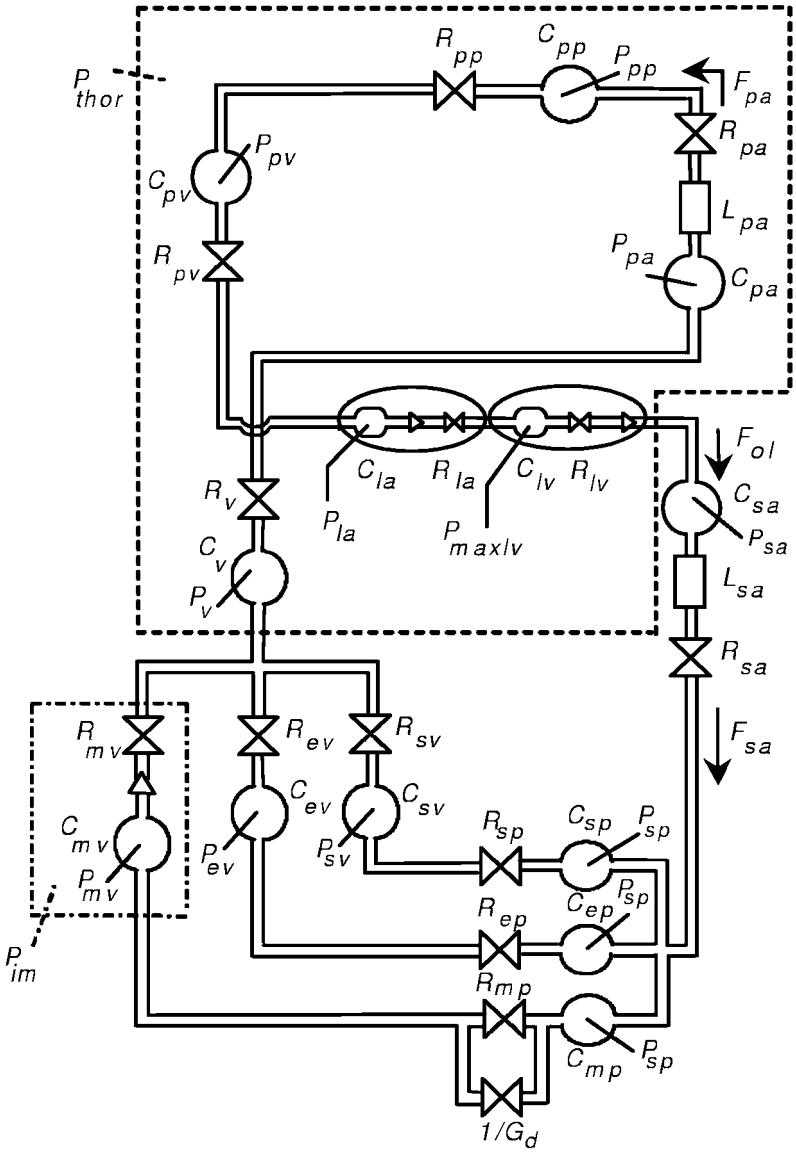

Fig. 2. Hydraulic analog of the cardiovascular system in a patient with cavopulmonary connection. Pulmonary arteries have been coupled directly to systemic veins. The meaning of the symbols is the same as in Fig. 1.

The baroreceptor control mechanisms. The baroreflex model is the same in both circulatory models. In fact, experiments of lower body negative pressure (LBNP) suggest that univentricular patients have an intact baroreceptor response (15). The model distinguishes among the afferent pathways from arterial and cardiopulmonary baroreceptors, the efferent (sympathetic and vagal) activities, and the responses of several distinct effectors (see block diagram in Fig. 3).

Afferent information from arterial baroreceptors is described by accounting for both static and rate-dependent gains in series with a sigmoidal function. As has been shown in a previous work (40), this representation allows for a fairly good replication of experimental results on baroreceptor stimulation.

The model of the cardiopulmonary baroreceptors, not included in our previous studies, is based on the series arrangement of a low-pass filter (which reproduces baroreceptor dynamics) and a sigmoidal relationship with lower threshold and upper saturation (see *Eqs. A5* and A*6* in the APPENDIX). Because these receptors are mainly located in the left atria and pulmonary veins, transmural pressure at pulmonary veins was used as their input quantity.

The efferent pathways include both sympathetic and parasympathetic divisions. Vagal activity to the heart is a nonlinear function of arterial baroreceptor activity and of cardiopulmonary activity (*Eqs. A10* and *A11* in the APPENDIX). Distinct equations were used to describe sympathetic activity to peripheral resistance, to the veins, and to the heart. According to experimental results, the frequency of the sympathetic discharge is a decreasing function of afferent activity, whereas the latter is computed as the weighted sum of the activity from arterial and cardiopulmonary baroreceptors (see *Eqs. A8* and *A9* in the APPENDIX). However, because the role of arterial and cardiopulmonary baroreceptors is dissimilar in the control of peripheral resistance, venous unstressed volume, and heart period, different weights were used to compute the sympathetic activity directed to the peripheral arterioles, to the venous circulation, and to the heart.

The model includes four different effectors to fulfil the regulatory actions. Three of them (heart contractility, peripheral systemic resistance, and systemic venous unstressed volume) change in response to sympathetic stimulation alone. In particular, an increase in the frequency of the efferent sympathetic nerves causes an increase in peripheral

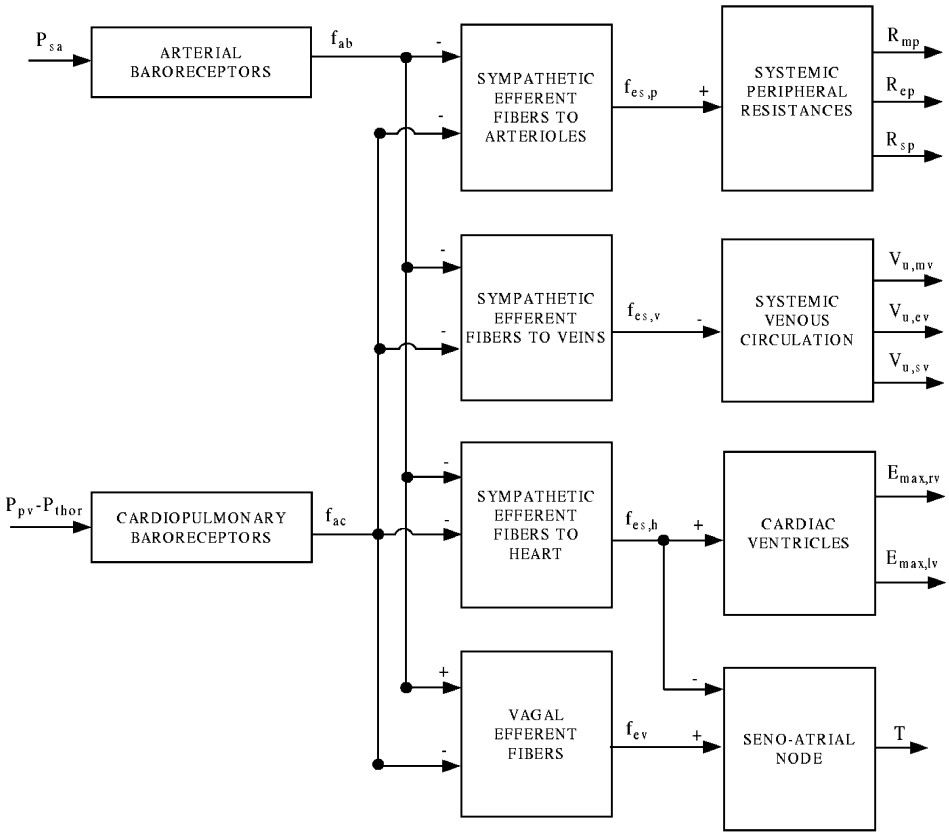

Fig. 3. Block diagram showing the baroreflex regulatory actions according to the present model. P_{sa}, arterial pressure; $P_{pv} - P_{thor}$, transmural pressure at pulmonary veins; f_{ab}, afferent activity from arterial baroreceptors; f_{ac}, afferent activity from cardiopulmonary baroreceptors; $f_{es,j}$ (j = p, v, h), frequency discharge in efferent sympathetic activity to arterioles, to veins, and to heart, respectively; f_{ev}, discharge frequency in the vagus; R_{ep}, R_{sp}, R_{mp}, extrasplanchnic, splanchnic, and active muscle peripheral resistance; $V_{u,ev}$, $V_{u,sv}$, $V_{u,mv}$, extrasplanchnic, splanchnic and active muscle venous unstressed volume; $E_{max,RV}$ and $E_{max,LV}$, right ventricular and left ventricular end-systolic elastance; T, heart period.

systemic resistances (splanchnic, muscular, and extrasplanchnic) in end-systolic elastance, but a decrease in systemic venous unstressed volumes (splanchnic, muscular, and extrasplanchnic). The control of the heart period involves a balance between the sympathetic and parasympathetic efferent activities: the heart period decreases by rising the frequency of sympathetic fibers, whereas it increases rising the frequency of spikes in the vagus. In the model we assumed a simple linear interaction between the two heart period control mechanisms because this choice can reproduce several experimental data quite well (20).

Response to moderate dynamic exercise. During exercise, the cardiovascular system is challenged to supply the increased metabolic needs of working muscles while at the same time maintaining the requirements of other essential organs. This is achieved by an increased pulmonary ventilation, an increased CO, a slight hypertension, and a redistribution of blood flow toward the active muscles (5, 33). These cardiovascular adjustments result from the superimposition between local vascular control mechanisms and a reconfiguration of autonomic neural activity; in particular, sympathetic activity to the heart and blood vessels is increased while parasympathetic activity to the heart is decreased. Several experimental results support the idea that motor command from the cerebral cortex, besides initiating movements, activates the autonomic nervous system (either directly or through a shift in the baroreceptor characteristic) (9, 18). Furthermore, it seems likely that the central command plays a major role during mild and moderate exercise, whereas during severe exercise afferent information from muscle receptors also affects cardiovascular response (5, 33). In this study, only moderate exercise was considered, therefore, no other reflex mechanism was introduced. The central motor command has been reproduced through offset terms in sympathetic and vagal activities (see *Eqs. A8* and *A10* in the APPENDIX).

The increase in muscle blood flow during exercise has been ascribed to two concurrent mechanisms: metabolic vasodilation and the effect of the so-called "muscle pump." The first mechanism has been mimicked by reducing the peripheral resistance in the leg skeletal muscle. To this end, a parallel conductance in the skeletal muscle compartment of the leg was inserted (see Figs. 1 and 2). Naturally, this conductance value depends on exercise intensity. The effect of the active muscle pump has been mimicked assuming that, during dynamic exercise, extravascular pressure for the muscle veins (i.e., intramuscular pressure, P_{im}, in Figs. 1 and 2) oscillates between 0 and a positive level with a rhythmic pattern (*Eqs. A13–A15* in the APPENDIX) (31). Moreover, the pressure-volume characteristic of the muscle veins (hence, venous compliance) have been given two different expressions, depending on whether transmural pressure is positive or negative. At positive values of transmural pressure the classic linear pressure-volume relationship was used, i.e., constant compliance, where the x-axis intercept defines the unstressed volume. In contrast, at negative levels of transmural pressure a nonlinear relationship of collapsing tubes taken from Pedley (29) was adopted (*Eq. A1*). This relationship implies that the veins become extremely elastic during collapse, thus resulting in the expulsion of blood volume. Because of the presence of valves (*Eq. A2*), this intermittent venous squeezing during dynamic exercise favors venous return and CO.

To reproduce the increase in frequency and depth of breathing, parameters characterizing the pattern of intrathoracic pressure have been changed accordingly (11, 23, 37, 41). Dependence of the central command and muscular vasodilation parameters (i.e., the offset terms in sympathetic

and vagal activities and peripheral conductance of the skeletal muscle vascular bed of the leg) on the intensity of exercise has been given to simulate the response of a normal subject to exercise (see RESULTS).

For the sake of simplicity, a possible involvement of the myogenic response to sustain hypertension during exercise, as observed by Lash and Shoukas (17), was not included explicitly in this work; hence, all experimental vasoconstriction is ascribed to sympathetic influences alone.

Simulated conditions. The model has been used as follows. First, to assign a value to the parameters describing cardiopulmonary baroreceptors, we preliminarily simulated the response of the main hemodynamic quantities (MAP, CO, and HR) in the NC to different levels of LBNP. Subsequently, hemodynamics at rest have been compared in the NC and the UC using the basal parameter values (40). Because the values of CO and MAP in the UC patient were too low compared with the literature, a sensitivity analysis was performed on the key cardiovascular parameters to recognize which parameter changes may allow for the restoration of more acceptable hemodynamics in the single pump circulation. Finally, the response to moderate exercise was simulated, both in the NC and the UC patient, taking suggestions from the sensitivity analysis into account.

RESULTS

Simulation of LBNP. The values of the parameters that characterize the cardiopulmonary baroreflex (i.e., parameters in the static sigmoidal relationship, *Eq. A6*, and the weighting factors in the expressions of sympathetic and vagal activity, *Eqs. A9* and *A11* of the APPENDIX) have been given to reproduce MAP, CO, and HR in normal humans at different levels of LBNP ranging between −10 and −50 mmHg. To simulate the effect of LBNP, it was assumed that any 10-mmHg depression around the legs causes a volume pooling as high as about 100 ml (4). This is the same as assuming a lower body venous compliance as high as 10 ml/mmHg, i.e., the compliance of the skeletal muscle compartment of the legs (C_{mv} = 6.6 ml/mmHg) augmented by a small portion (3.4 ml/mmHg) of the extrasplanchnic venous compliance.

Simulation results are shown in Fig. 4, whereas parameter numerical values are reported in Table 1. The agreement between model results and in vivo data (4, 24) is acceptable.

Comparison of normal and univentricular hemodynamics at rest. The mean values of the main cardiovascular quantities over the cardiac cycle, computed with the mathematical model of a normal subject at rest, are listed in the first column of Table 2. These data are considered as the reference conditions for a functioning biventricular circulation.

The second column shows the same quantities computed in the case of UC. The absence of the right pump results in an unloading of the baroreceptors (both cardiopulmonary and arterial), which respond by increasing sympathetic activity and decreasing vagal activity. As a consequence, splanchnic and extrasplanchnic resistances, heart rate and cardiac contractility (E_{max}) are increased in comparison with the reference case, whereas unstressed venous volumes are reduced. These compensatory actions, however, are insufficient in restoring the reference conditions (compare the first and second columns), i.e., the absence of the right heart can be only partially offset. In particular, MAP and pulmonary arterial pressure settle at a value significantly lower than normal. Despite the significant rise in HR, CO remains significantly low due to the peripheral vasoconstriction and, above all, due to insufficient venous return (proportional to the difference between pulmonary arterial pressure and left atrial pressure). In this regard, it can be observed that a comparison of venous return in NC and UC can be achieved by calculating the quantity $(P_{pa} - P_{la})/(R_{pa} + R_{pp} + R_{pv})$, where the numerator represents the overall perfusion

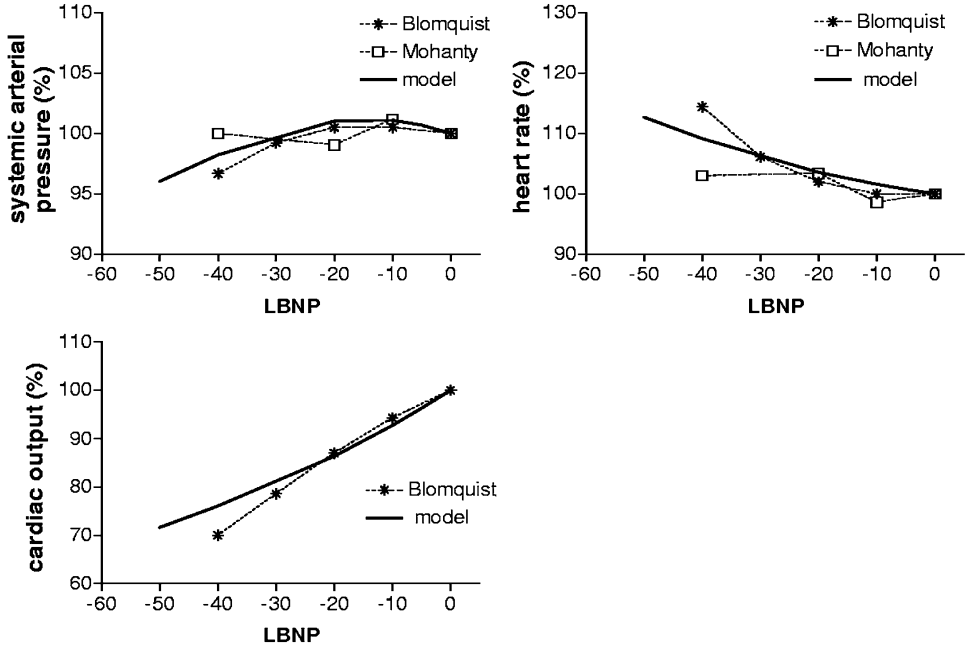

Fig. 4. Percentage changes of mean systemic arterial pressure, heart rate, and cardiac output (CO) simulated with the model in response to different levels of lower body negative pressure (LBNP, continuous line) and compared with in vivo data in normal volunteers (4, 24). In performing these simulations we assumed that venous compliance in the lower body is 10 ml/mmHg.

Table 2. *Results of sensitivity analysis*

	NC	UC	UC ($V_{u,sv}$, $V_{u,ev}$, $V_{u,mv}$)	UC (V_t)	UC (C_{sv}, C_{ev}, C_{mv}, C_v)	UC ($E_{max,lv}$, $V_{u,lv}$)	UC (R_{sp}, R_{ep}, R_{mp})	UC (V_t, $E_{max,lv}$, $V_{u,lv}$)
MAP, mmHg	93.2	84.9	94.0	94.3	93.6	90.1	87.0	101.3
Systolic AP, mmHg	122.1	102.9	116.4	117.0	115.8	110.4	104.6	127.2
Diastolic AP, mmHg	81.4	78.4	85.6	85.8	85.3	82.8	80.7	91.7
P_v, mmHg	2.8	7.1	9.7	9.8	9.5	6.7	6.8	9.3
P_{pa}, mmHg	14.5	6.8	9.4	9.5	9.2	6.4	6.5	9.0
P_{pv}, mmHg	5.1	1.3	2.6	2.7	2.5	0.4	1.3	1.6
P_{la}, mmHg	4.6	1.0	2.3	2.3	2.2	0.1	1.0	1.2
P_{mcf}, mmHg	9.0	10.8	13.5	13.7	14.2	10.6	10.6	13.3
CO, ml/s	83.3	48.6	59.9	60.6	59.2	53.0	46.1	65.8
F_e, ml/s	58.3	32.3	40.4	40.9	39.9	35.3	30.3	44.4
HR, beats/min	74.8	90.4	78.8	78.3	79.2	84.9	87.4	73.8
$V_{u,sv}$, ml	1067.0	1022.5	733.6	1103.3	1097.8	1069.4	1044.6	1166.7
$V'_{u,ev}$, ml	1353.1	1330.9	1186.6	1371.2	1368.5	1354.3	1341.9	1402.9
$E_{max,lv}$, mmHg/ml	3.0	3.6	3.4	3.4	3.4	3.9	3.6	3.8
R_{sp}, mmHg·s·ml^{-1}	3.4	4.5	4.1	4.0	4.1	4.4	4.8	4.0
R'_{ep}, mmHg·s·ml^{-1}	1.4	2.3	2.0	2.0	2.0	2.3	2.6	2.0

Each column includes the simulated mean value of the main cardiovascular variables. NC, normal circulation; UC, univentricular circulation; MAP, mean arterial pressure; AP, arterial pressure; P_v, pressure in systemic thoracic veins; P_{pa}, pulmonary arterial pressure; P_{pv}, pulmonary venous pressure; P_{la}, left atrium pressure; P_{mcf}, mean circulatory filling pressure; CO, cardiac output; F_e, total extrasplanchnic flow; HR, heart rate; $V_{u,sv}$, splanchnic venous unstressed volume; $V'_{u,ev}$, total extrasplanchnic venous unstressed volume (i.e., $V_{u,ev} + V_{u,mv}$); $E_{max,lv}$, left ventricle end-systolic elastance; R_{sp}, splanchnic peripheral resistance R'_{ep}, total extrasplanchnic peripheral resistance (i.e.; the parallel of R_{ep} and R_{mp}); V_t, total blood volume; C_{sv}, C_{ev}, C_{mv}, C_v, splanchnic and extrasplanchnic venous compliance, compliance of active muscle veins and compliance of systemic thoracic veins; $V_{u,lv}$, x-axis intercept of the left ventricle end-systolic pressure-volume curve. First column refers to a normal subject (NC) in resting conditions, when all model parameters have their basal value (40). Other columns refer to a univentricular patient (UC). Second column refers to circulation simulated with all the parameters at their basal value. Columns from third to eighth refer to the simulation repeated by individually modifying the quantities indicated in parentheses in the corresponding heading. See APPENDIX for details.

pressure of the pulmonary vascular bed and the denominator is the overall pulmonary resistance. Because the latter term is kept equal in NC and UC in the present study, venous return differences can be ascribed to differences in the numerator only.

The values of MAP and CO in the second column of Table 2 are insufficient compared with the values that can be found in the clinical literature. Clinical studies (15, 42) suggest that MAP in UC at rest is normal or even slightly increased (mainly due to an increase in diastolic pressure), whereas CO is about two-thirds normal. To achieve hemodynamic values in UC in closer agreement with the clinical literature, we assumed that univentricular hemodynamics is maintained not only by baroreflex activation, but also by a chronic alteration in some parameters. These alterations may reflect the action of long-term regulation mechanisms, not considered explicitly in the present model. To support this assumption, the UC was simulated by individually modifying: *1*) each of the major factors governing mean filling pressure, i.e., venous unstressed volumes (Table 2, *column 3*), total blood volume (*column 4*), and venous compliances (*column 5*); *2*) the left ventricular contractility described by means of the end-systolic pressure volume relationship (*column 6*); and *3*) the peripheral systemic resistances (*column 7*). However, the end-systolic elastance, unstressed volumes, and peripheral resistances in the model are not constant parameters but are actively controlled by the sympathetic nerve fibers. Hence, to modify the latter quantities, the static characteristics "parameter value versus sympathetic activity" were shifted to the left. These changes mimic a chronic alteration in the effector response. A more accurate description of the parameter changes performed during the sensitivity analysis can be found in the APPENDIX.

As expected, permanent variations in the quantities affecting mean filling pressure (Table 2, *columns 3–5*) cause an increase in MAP and especially in CO because of an increase in venous return. In particular, noteworthy is the increase in pulmonary arterial pressure. However, the price to be paid is a significant increase in systemic venous pressure that, in accordance with clinical data (12), is significantly higher than the value observed in NC (14).

The simulated increase in the left ventricle contractility (*column 6* of Table 2) causes a mild benefit to CO compared with the previous cases and only a partial restoration of the MAP level. Moreover, it should be noted that greater increases in the E_{max} parameter provide only negligible further improvements.

Finally, the increase of peripheral resistances in both the extrasplanchnic (R_{ep}), leg skeletal muscles (R_{mp}), and splanchnic (R_{sp}) districts (see *column 7* of Table 2) causes only a small increase in MAP. Moreover, this result is obtained through a dramatic fall in CO (down to 46 ml/s). The latter result was well expected and agrees with clinical observations (1).

Of course, the increase in end-systolic elastance has greater benefits when it is paralleled by an increase in venous return. For this reason, the effect of a simultaneous increase in total blood volume and end-systolic characteristic was tested in the last column of Table 2 by combining the parameter changes separately used in *columns 4* and *6*. Results show that an increase in cardiac contractility may be efficacious toward improv-

ing MAP and CO, provided it is supported by an increase in venous return (compare results in Table 2, *columns 8* and *6*). However, the latter condition is unlikely in UC for two reasons. First, clinical and theoretical studies suggest that cardiac contractility is depressed rather than enhanced in patients with UC (1, 26). Second, results in the last column of Table 2 show an increase in systolic arterial pressure. The latter result is in disagreement with clinical data (15).

In conclusion, the sensitivity analysis suggests that the achievement of hemodynamic values in the UC patients in agreement with the clinical literature can be ascribed to a chronic shift in a parameter affecting mean filling pressure combined with the regulatory action of the cardiopulmonary baroreceptors (which are triggered by the decrease in pulmonary venous pressure). Arterial baroreceptors play a minor role and are activated only if the previous compensations fail to maintain normal systemic arterial pressure.

Response to moderate exercise. Simulation of moderate exercise was performed by considering two levels of oxygen consumption rate ($\dot{V}O_2$, 1 and 2 l/min). The values of the parameters that simulate dynamic exercise (i.e., the shift in the sympathetic and vagal activities, $f_{es,cc}$ and $f_{ev,cc}$, see *Eqs. A8* and *A10* in the APPENDIX, and the increase in active muscle conductance, G_d) have been tuned so that simulation results on the normal subject agree with experimental data (28) (Fig. 5). Moderate exercise is accompanied by a large increase in CO, an increase in HR, and a dramatic fall in systemic peripheral resistance. The decrease in systemic peripheral resistance is mostly due to muscle vasodilation and counters the increase in systemic arterial pressure; as a consequence, arterial pressure only rises modestly.

Figure 6 shows the results of four different cardiovascular responses to moderate exercise (1 l/min) simulated in the univentricular subject, presupposing the occurrence, at rest, of no compensation and of one of the three compensations on mean filling pressure analyzed in Table 2 (*columns 3–5*). The case analyzed in *column 7* (i.e., a change in peripheral resistances) was not examined because of its poor effectiveness in maintaining basal CO. The increase in E_{max} (either alone or with a simultaneous increase in blood volume, *columns 6* and *8*) was not simulated because univentricular patients seem to have depressed rather than augmented contractility (1, 26). To facilitate the comparison, the simulated cardiovascular adjustments in a normal subject are repeated in each histogram. Moreover, all quantities are normalized to the value occurring in the normal subject at rest (assumed to be 100%).

As clearly shown in Fig. 6, a decrease in venous unstressed volume (V_{uv}) is the compensation that results in the worsened CO response to moderate exercise. In fact, a chronic decrease in V_{uv} implies that the venous system has already mobilized part of its blood reserves, thus a smaller amount of blood is available to be displaced in response to physiological stress. The CO exhibits a greater increase in the other two kinds of resting compensation. In particular, we can observe that an elevated stiffness in the venous wall (i.e., reduced compliance) allows CO to be sustained during exercise better than an elevated total blood volume.

Figure 7*A* depicts CO as a function of exercise intensity, quantified by the $\dot{V}O_2$. The shaded area represents the normal value range experimentally obtained in a control group (42). The symbols show our simulation results on normal subject and on a UC patient with the three different kinds of resting compensation. The model predictions for the normal subject fall into the experimental range. Predictions obtained in the UC are also in acceptable agreement with clinical data (42). In all three cases examined, CO at rest falls into the normal range, although below the median line. At a moderate exercise level (1 l/min) CO in the UC still lies within the normal range. However, when $\dot{V}O_2$ exceeds 1.2–1.3 l/min, UC patients become unable to significantly increase CO, mainly due to an insufficient venous return. The model results quite well agree with clinical data by Zellers et al. (42) (Fig. 7*B*).

Starting from data in Fig. 7, it is possible to approximately evaluate a threshold between aerobic and anaerobic metabolism during exercise. During exercise, in fact, arteriovenous oxygen difference may increase up to ~0.16 ml O_2/ml blood (19). Assuming such an elevated oxygen extraction, an upper bound $\dot{V}O_{2\,max}$ for the oxygen consumption rate (that is CO multiplied by arterovenous oxygen difference) can be computed as $\dot{V}O_2 \leq 0.16 \cdot CO = CO/6.25 = \dot{V}O_{2\,max}$. Accordingly, the threshold between aerobic and anaerobic metabolism (i.e., the point when $\dot{V}O_2 = \dot{V}O_{2\,max}$) can be approximated in Fig. 7 by the following equation $CO = 6.25 \cdot \dot{V}O_2$. This is the equation of a straight line passing through the origin and through the point of coordinates (1, 6.25). As clearly shown in Fig. 7, at a moderate exercise level ($\dot{V}O_2$ = 1.0 l/min) oxygen extraction to the

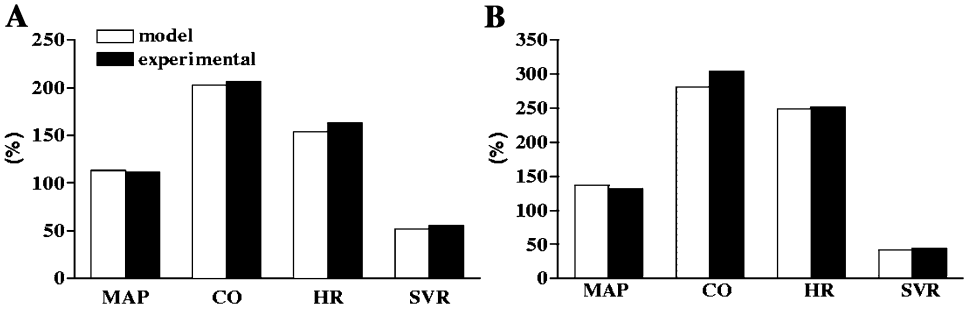

Fig. 5. Values of mean arterial pressure (MAP), CO, heart rate (HR), and systemic vascular resistance (SVR) simulated with the model at two different levels of dynamic exercise, corresponding to an overall oxygen consumption rate as high as 1 (*A*) and 2 l/min (*B*), respectively. All quantities are expressed as percentages of the basal value occurring in a normal subject in resting conditions. Experimental data (28) refer to normal subjects.

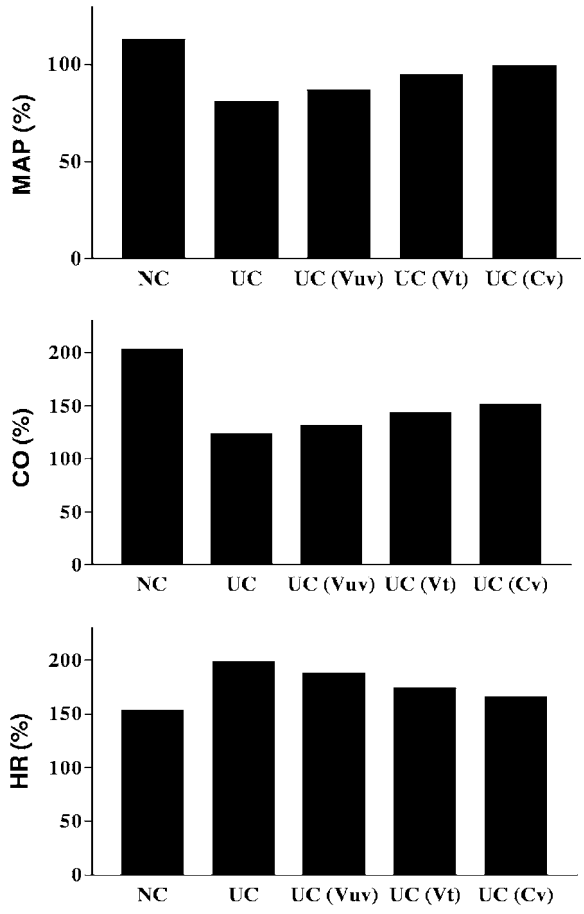

Fig. 6. Comparison between model simulation response to moderate exercise [O_2 consumption ($\dot{V}O_2$) = 1 l/min] in the normal subject (NC) and in the univentricular patient without any compensation (UC) and for the three most efficient compensations presented in Table 2 [reduced venous unstressed volume: UC (V_{uv}); increased total blood volume: UC (V_t); reduced venous compliance: UC (C_v)]. All the quantities are expressed as percentages of the basal value occurring in a normal subject in resting conditions.

active muscle in UC can still sustain the $\dot{V}O_2$, because oxygen delivery may surpass the $\dot{V}O_2$. By contrast, when $\dot{V}O_2$ exceeds 1.2–1.3 l/min, oxygen extraction in UC patients becomes inadequate to the $\dot{V}O_2$ (dashed lines in Fig. 7), and the patient must rely on anaerobic metabolism.

DISCUSSION

It is well documented that the recipients of Fontan circulation exhibit quite a normal systemic arterial pressure, a moderate reduction in CO and stroke volume, but an elevated venous pressure at rest. This hemodynamic scenario allows for a basal functioning of the cardiovascular system but becomes dangerously critical in response to exercise compared with healthy subjects. This impairment is mainly evident in the insufficient capacity to increase stroke volume and hence CO (42). Although the previous aspects have been well documented (2, 15, 36, 42), a clear understanding of the phenomena involved and the role of individual hemodynamic factors is still lacking.

To achieve a deeper understanding of hemodynamic adjustments in patients with cavopulmonary connection, both at rest and during moderate exercise, a modified mathematical model of cardiovascular dynamics, integrated with the arterial and cardiopulmonary baroreflex system, was used in the present work.

Several computer models of the cardiovascular system in subjects with univentricular heart have been proposed in recent years with different purposes. The model developed by Pennati et al. (30) has been used in particular to investigate local hemodynamics at the reconstructive junction for the purpose of optimizing the surgical procedure and reducing the postoperative risks for the patient. Other mathematical models (16, 34) have been constructed to analyze the effect of changes in some cardiovascular parameters on systemic hemodynamics in this type of circulation. Nevertheless, none of these models incorporates a detailed

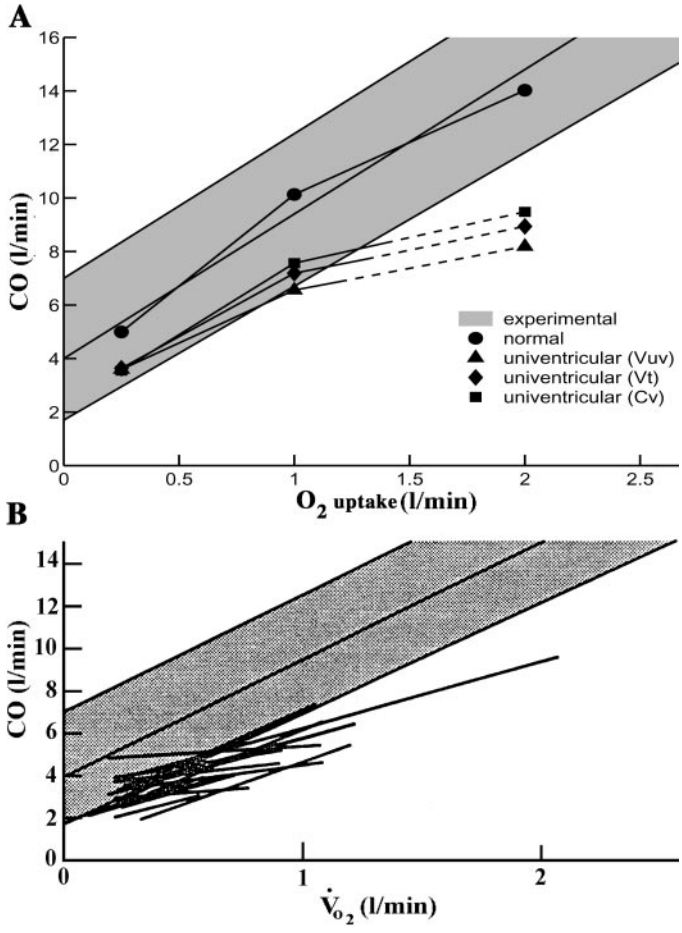

Fig. 7. Static relationship between CO and $\dot{V}O_2$ rate. *A*: simulation results. Circles, rest and exercise CO obtained with the model simulating a normal subject. Triangles, rhombi, and squares, rest and exercise CO obtained with the univentricular model simulating the three resting compensations shown in Table 2 (V_{uv}, V_t, and C_v, respectively). Dashed lines represent the portions of the curves where O_2 delivery to the muscle does not warrant aerobic metabolism. Shaded area between broken lines, normal range of values experimentally obtained on a control group (from Ref. 42). *B*: redrawn from data measured by Zellers et al. (42) in normal subjects (shaded area) and in 18 Fontan patients.

description of regulatory feedback mechanisms such as the arterial and cardiopulmonary baroreflex. The latter modulate several cardiovascular parameters and may thus contribute significantly to the responses observed in vivo.

Here the results obtained at rest will be discussed first. Subsequently, new hypotheses on the response to moderate exercise will be outlined below.

Hemodynamics of univentricular patients at rest. The first simulation was performed by simply removing the right heart from the model and computing the consequent values of hemodynamic quantities; results suggest that a single heart in series with the entire circulation cannot assure proper hemodynamics, even when physiological baroreflex compensation and the respiration effect on venous pulsatility are considered. The model revealed that the main cause behind this deterioration in hemodynamics is the insufficient venous return, which abates stroke volume, and thus CO and systemic arterial pressure. Consequently, we performed a sensitivity analysis to evaluate which chronic changes should take place to restore hemodynamic data more similar to those clinically observed in univentricular patients. This analysis demonstrated that the compensation able to produce hemodynamic in close agreement with that occurring in univentricular patients at rest is a moderate chronic alteration in a parameter affecting the mean filling pressure, reinforced by the response of cardiopulmonary baroreceptors. The latter cause a significant increase in systemic resistance and a moderate increase in heart rate.

The increase in mean filling pressure required to reproduce hemodynamics in univentricular patients is probably the result of additional long-term adjustments not considered in the present model. This increase can be achieved by means of different alternative strategies: increasing total blood volume (perhaps by means of capillary fluid reabsorption and renal regulation), reducing venous unstressed volume [which might occur via a long-term increase in venous vessel tone, perhaps through sympathetic influences (32, 38)], or reducing venous compliance (which might reflect alterations in venous wall mechanical properties).

Arterial baroreceptors seem to play a minor role in univentricular patients at rest, because the combined action of cardiopulmonary baroreceptors and the long-term increase in mean filling pressure permit the restoration of a normal MAP level (15). Still, a certain effect of arterial baroreceptors may ensue from the decrease in pressure pulsatility (see Table 2 and Ref. 15); in fact, these receptors are sensitive not only to the instant arterial pressure level, but also to the rate of change of pressure waveform (40).

Results of the previous sensitivity analysis agree with the theoretical and clinical findings by Kresh et al. (16). These authors, with a simple computer model and animal experiments, reached the conclusion that near-normal blood flow in the absence of the right heart can be warranted only by an increase in stressed blood volume or by a selective reduction in systemic venous compliance. More recently, Macé et al. (21), through experiments in anesthetized pigs, observed that mean circulatory filling pressure must be elevated in Fontan versus biventricular circulation (21.8 ± 1.3 vs. 10.6 ± 0.8 mmHg) to achieve comparable values of systemic blood flow. The authors analyzed their data in terms of the Guytonian relationship among CO, mean circulatory filling pressure, and venous return. These results agree with those shown in Table 2 of the present work (*columns 3–5*) thinking that the compensations on mean circulatory filling pressure accomplished during the sensitivity analysis (P_{mcf} in the range of 13.5–14.2 mmHg) allow for only a partial restoration of the basal CO level.

This scenario is supported by the clinical data reported by Kelley et al. (15). These authors observed that Fontan subjects have a reduced venous capacitance (as measured by forearm venous congestion or LBNP), increased forearm vascular resistance, increased HR, and elevated resting plasma norepinephrine levels compared with control subjects. Hence, the activity of the noradrenergic sympathetic nervous system appeared elevated in these patients and venous tone appeared higher than normal. Furthermore, data by Kelley et al. (15) suggest that arterial pressure pulse amplitude is reduced in Fontan versus biventricular subjects, especially due to a reduction in systolic pressure, while diastolic pressure is moderately elevated. As a consequence, MAP unchanged or mildly increased and pressure pulsatility reduced. The latter observation agrees with results in *columns 3–5* of Table 2.

Response to moderate exercise. According to the observations reported in clinical studies, the simulated response to moderate exercise in UC is considerably reduced compared with NC, especially when $\dot{V}O_2$ increases above 1 l/min (2, 36, 42). In particular, results of Fig. 6 suggest that univentricular patients have a greater HR but reduced CO during moderate exercise compared with normal subjects, hence, they have lower stroke volume. Furthermore, the present model predicts that univentricular patients can have a maximum $\dot{V}O_2$ for aerobic metabolism as high as ~1.2–1.3 l/min, depending also on the type of compensation adopted, whereas normal subjects can increase $\dot{V}O_2$ up to 2 l/min without reaching the anaerobic threshold. The latter predictions agree with clinical data quite well (8, 39, 42).

However, the interpretation provided by the model is quite different from the one usually reported in the literature. Generally, a depressed CO response to exercise is ascribed to heart factors, such as impaired ventricular function, abnormal activity in the sinus node, or abnormal conduction (2). Zellers et al. (42) hypothesized that a single systemic ventricle may frequently be compromised by prolonged hypoxemia and/or chronic volume overload. Vascular factors affecting preload have also received attention as a potential cause of the abnormal stroke volume responsiveness. Shachar et al. (36) measured an increased pressure gradient in the conduit between the right atrium and the pulmonary arteries during exercise in patients 4–25 mo after the operation. Hence, they

concluded that conduit obstruction may have contributed to a poor cardiac response to exercise in these subjects. The present study suggests a further possible mechanism for the reduced response to exercise. Simulation results, reported in Figs. 5–7, have been obtained by considering normal characteristic for the left ventricle and normal pulmonary hemodynamic parameters. Hence, none of the hypotheses mentioned above has been incorporated in the model. In contrast, results suggest that a subnormal stroke volume increase to moderate exercise may be the consequence of an insufficient increase in mean filling pressure to sustain venous return, which in turn results in a poor stroke volume response and insufficient CO increase. To test this hypothesis, it may be of value to measure the difference $P_{pa} - P_{la}$ in UC, especially in conditions of increased CO demand.

The insufficient capacity of univentricular patients to increase venous return and stroke volume is the consequence of various concurrent phenomena. First, univentricular patients exhibit an increase in the resistance to venous return, which includes the series arrangement of the systemic and pulmonary vascular beds. Hence, even if the systemic resistance decreases dramatically during exercise, the resistance to venous return is still quite elevated due to the series arrangement of the pulmonary vascular bed. Of course, this result strictly depends on the assumption that pulmonary resistance does not vary significantly during exercise, i.e., pulmonary vessel recruitment is already maximal at rest. Second, systemic resistance is elevated in univentricular patients due to vasoconstriction of peripheral arterioles caused by the baroreflex control. This phenomenon contributes to a reduced CO (1). Finally, to simulate the hemodynamics of univentricular patients at rest, we assumed a chronic shift in a parameter affecting mean filling pressure. As a consequence of this adjustment, the venous vascular bed may have exploited or attenuated its blood volume compensation reserve; i.e., it may possess a smaller capacity to further mobilize blood volume. Among the three permanent alterations tested in Figs. 5–7 (i.e., the shift in the unstressed volume characteristic, the increase in total blood volume, or the decrease in venous compliance), a shift in the venous unstressed volume causes the more precocious exhaustion of the compensatory reserve; as in this case the increase in sympathetic activity during moderate exercise can only produce a minimal additional decrease in unstressed volume. By way of contrast, a reduction in venous compliance warrants a more extended compensation. Indeed, if compliance is reduced, the increase in stressed blood volume caused by sympathetic activation occurs against a more rigid venous compartment; this leads to a greater pressure rise and improved venous return. Even in this more favorable case, however, the capacity of univentricular patients to increase venous return and CO appears lower during exercise compared with NC.

Of course, the previous explanation supported by model simulations does not exclude the possibility that other phenomena, such as impairment in left ventricle performance or obstruction in the cavopulmonary conduit, may further contribute to the reduced exercise response. In this regard, it can be observed that CO in UC during exercise is still a little higher in the present simulations than in clinical data (compare *A* and *B* of Fig. 7). One can expect that a reduction in heart contractility [i.e., a reduction in E_{max} and/or a right shift in the end-systolic characteristic, as observed in some univentricular patients (1)] may further abate the response to exercise, thus providing even better agreement between model and clinical observations. Reduced response to exercise is presumably a multifactorial phenomenon caused by different factors acting together; i.e., insufficient venous return, depressed heart contractility, increased resistances, etc.

An important drawback to the present study concerns the limited comparison between model predictions and real data in the literature. Unfortunately, existing data to support model predictions are in very short supply and concern only a few hemodynamic parameters. Performing a deeper comparison would be of great value in future works to confirm the validity of the main model assumptions or to discover aspects that require improvement or modifications. This comparison, however, calls for important hemodynamic quantities to be monitored in UC patients, both at rest and during moderate exercise. Among the main model assumptions, which need extensive validation, we can mention the constancy of pulmonary resistance, the maintenance of an adequate cardiac contractility, and the direct coupling between the systemic veins and pulmonary arteries, which can mimic only certain types of Fontan procedures.

In conclusion, the present study suggests that relatively normal hemodynamics in patients with cavopulmonary connection at rest may be sustained by a combination of increased sympathetic activity (possibly caused by baroregulation), associated with a permanent change in a parameter affecting mean filling pressure (venous unstressed volume decrease, an increase in total blood volume, compliance decrease). Moreover, the response to moderate exercise is depressed compared with normal subjects, because the UC patients may fail to raise the venous return to a level capable of supporting CO and the oxygen consumption rate. This deficit can be ascribed to an elevated resistance to venous return and/or to a reduced capacity to mobilize blood volume and increase mean filling pressure. This phenomenon, together with other possible mechanisms (such as a depressed cardiac contractility), can explain the pathophysiology of UC.

APPENDIX

The Cardiovascular System

The main changes introduced in the cardiovascular system modeling compared with the previous work (40) are *1*) the inclusion of a new subsystem (subscript v), which mimics venous segment traversing the thorax; *2*) the division of the extrasplanchnic systemic circulation [which was a single

compartment in a previous model (40)] into the parallel arrangement of two distinct segments, representing the circulation in the active skeletal muscle (subscript m) and the circulation in all the remaining extrasplanchnic vascular beds (subscript e); and *3*) the periodic changes in transmural pressure at the vessels inside the thoracic cavity (Figs. 1 and 2) caused by respiration.

The thoracic venous segment includes a compliance (C_v) and a hydraulic resistance (R_v). The value of R_v has been chosen to have a very small pressure drop (≃0.5 mmHg) in the thoracic veins. The value of C_v has been given assuming that thoracic veins account for about one-third of the total systemic venous compliance (3). Compared with the previous model version (40), values of total extrasplanchnic and splanchnic venous compliance have been modified so that total venous compliance provides the same value as used in the previous study (i.e., 111.11 ml/mmHg) (see Table 1 for numeric values).

The subdivision of extrasplanchnic circulation has been performed assuming that the active muscle branch reproduces skeletal muscle in the legs. This choice is justified because pedaling exercise on a cycle ergometer is the test commonly used in the clinical practice to assess cardiopulmonary performance. Individual parameters of the new two branches m and e, in basal resting conditions, have been assigned considering that normal blood flow entering the skeletal muscle in the legs is ~13% of total CO (31) (thus blood flow in the remaining extrasplanchnic vascular beds is ~57% of CO) and that the ratio between analogous parameters in the two segments is the same as between flows. Finally, the parallel arrangement of the two segments provides the parameter values for the overall extrasplanchnic circulation. Because strong intramuscular contractions during exercise may cause veins to collapse (the so-called "muscle pump"), the relationship between transmural pressure and blood volume in the active muscle veins has been reproduced using the equations proposed by (29) for collapsible tubes

$$P_{mv} - P_{im} = \begin{cases} C_{mv} \cdot (V_{mv} - V_{u,mv}), & V_{mv} > V_{u,mv} \\ P_0 \cdot \left[1 - \left(\dfrac{V_{mv}}{V_{u,mv}} \right)^{-3/2} \right], & V_{mv} < V_{u,mv} \end{cases} \quad (A1)$$

where P_{mv} is the pressure inside the active muscle veins and P_{im} is the extravascular pressure of the active muscle veins (i.e., the intramuscular pressure). The latter is null under resting conditions, whereas it changes periodically during exercise (see *Simulations of exercise conditions*). V_{mv} is the total blood volume (stressed + unstressed) in the active muscle veins, $V_{u,mv}$ is the unstressed volume, C_{mv} represents the venous compliance in the active muscle compartment, and P_0 is a constant parameter. According to Pedley (29), P_0 is computed as $P_0 = V_{u,mvn}/(C_{mv} \cdot 10)$, where $V_{u,mvn}$ is the basal value of unstressed volume in active muscle veins. Furthermore, venous valves in the active muscle compartment, which prevent a retrograde flow during muscular contractions, are mimicked by an ideal diode arranged in series with the hydraulic resistance of active muscle veins (R_{mv}) (Figs. 1 and 2). Hence, the blood flow leaving the muscle ($F_{o,m}$) depends on the opening of the venous valve through the following equation

$$F_{o,m} = \begin{cases} 0, & \text{if } P_{mv} \le P_v \\ \dfrac{P_{mv} - P_v}{R_{mv}}, & \text{if } P_{mv} > P_v \end{cases} \quad (A2)$$

where P_v is pressure inside the thoracic veins.

Intrathoracic pressure in the model changes periodically according to the following equations

$$P_{thor}(t) = \begin{cases} P_{thor,max} - (P_{thor,max} - P_{thor,min}) \cdot \dfrac{T_{resp}}{T_i} \cdot s, \\ P_{thor,max} - \dfrac{(P_{thor,max} - P_{thor,min})}{T_e} \cdot (T_i + T_e - s \cdot T_{esp}), \\ P_{thor,max}, \end{cases}$$

$$0 \le s \le \frac{T_i}{T_{resp}}$$
$$\frac{T_i}{T_{resp}} \le s \le \frac{T_i + T_e}{T_{resp}} \quad (A3)$$
$$\frac{T_i + T_e}{T_{resp}} \le s \le 1$$

where T_{resp} is the respiratory period, T_i is the inspiration time, T_e is the expiration time, $P_{thor,min}$ is the value of intrathoracic pressure at the end of inspiration, whereas $P_{thor,max}$ is the value of the intrathoracic pressure at the end of the expiration and during the respiratory pause. s is a dimensionless variable ranging between 0 and 1 that represents the fraction of the respiratory cycle. The value $s = 0$ conventionally corresponds to the beginning of the inspiration. An expression for $s(t)$ has been obtained by using an additional state variable, $\epsilon(t)$

$$\frac{d\varepsilon}{dt} = \frac{1}{T_{resp}} \quad \text{with} \quad s(t) = \text{frac}(\varepsilon) \quad (A4)$$

where the function "fractional part" [frac( )] resets the variable $s(t)$ to zero as soon as it reaches a value of +1. According to clinical data (11, 23, 25, 37, 41), different values have been assigned to the parameters T_{resp}, T_i, T_e, $P_{thor,max}$, and $P_{thor,min}$ at rest, during mild exercise ($\dot{V}O_2$ = 1 l/min), and during moderate exercise ($\dot{V}O_2$ = 2 l/min) (see Table 1).

The Baroreflex Control System

The model of the baroreflex control system includes the activity in the afferent fibers from high-pressure (arterial) baroreceptors, the activity in the afferent fibers from low-pressure (cardiopulmonary) baroreceptors, their integration at the central neural level, the activity in the efferent sympathetic pathways to the periphery and in the vagus nerve, and the response of several effectors. The latter include heart period, myocardium end-systolic elastance, peripheral resistances, and unstressed venous volumes in the three systemic compartments.

Afferent information from arterial baroreceptors is described by using the same equations as in Ref. 40. Hence, they are not reported again for the sake of brevity.

We assumed that the afferent activity from the cardiopulmonary receptors depends on transmural pressure at pulmonary veins through a first-order, low-pass filter in series with a sigmoidal static characteristic. Hence, the following equations have been used

$$\tau_l \cdot \frac{dP_l}{dt} = -P_l + (P_{pv} - P_{thor}) \quad (A5)$$

$$f_{ac} = \frac{f_{max,l}}{1 + \exp\left(\dfrac{P_{tn} - P_l}{k_l} \right)} \quad (A6)$$

where $P_{pv} - P_{thor}$ is the transmural pressure at the pulmonary veins, τ_l is the time constant of the real pole in the

low-pass transfer function, P_l is the output variable of the low-pass filter, f_{ac} is the frequency of spikes in afferent fibers from cardiopulmonary receptors, $f_{max,l}$ is the upper saturation of the frequency discharge (the lower saturation is assumed equal to zero), P_{tn} is the pulmonary venous transmural pressure at the central point of the sigmoid, and k_l is a parameter related to the slope of the static function at the central point. By denoting with G_l the gain at the central point of the sigmoid, the following expressions hold

$$G_l = \left.\frac{\partial f_{ac}}{\partial P_l}\right|_{P_l = P_{tn}} \qquad k_l = \frac{f_{max,l}}{4 \cdot G_l} \tag{A7}$$

The elaboration process at the central neural system has been reproduced assuming that activities coming from arterial and cardiopulmonary receptors are multiplied by constant gains and then summed. In accordance with the previous work (40), we assumed that the frequency of sympathetic discharge decreases exponentially with the overall afferent activity, whereas efferent vagal discharge increases monotonically with the overall afferent activity in a sigmoidal fashion. An important modification in the present study, compared with the previous one, is that we have distinguished between efferent sympathetic activity to peripheral vessels to the veins and to the heart. This choice is justified because experiments of LBNP can be reproduced reasonably well assuming a different sympathetic action on heart, venous unstressed volumes, and peripheral resistances. Hence, the following equations hold

$$f_{es,j} = f_{es,\infty} + (f_{es,0} - f_{es,\infty}) \cdot \exp(-k_{es} \cdot f_{a,j}) + f_{es,cc} \quad j = p, v, h \tag{A8}$$

$$f_{a,j} = G_{ab,j} \cdot f_{ab} + G_{ac,j} \cdot (f_{ac} - f_{ac,0}) \quad j = p, v, h \tag{A9}$$

$$f_{ev} = \frac{f_{ev,0} + f_{ev,\infty} \cdot \exp\left(\frac{f_{a,vag}}{k_{ev}}\right)}{1 + \exp\left(\frac{f_{a,vag}}{k_{ev}}\right)} - f_{ev,cc} \tag{A10}$$

$$f_{a,vag} = G_{ab,vag} \cdot (f_{ab} - f_{ab,0}) + G_{ac,vag} \cdot (f_{ac} - f_{ac,0}) \tag{A11}$$

$f_{es,j}$ (j = p, v, h) is the frequency of spikes in the efferent sympathetic fibers directed to the peripheral resistances, the veins, and the heart, respectively, f_{ab} is the afferent activity from arterial baroreceptors, f_{ac} is the afferent activity from cardiopulmonary baroreceptors (*Eq. A6*), $f_{ab,0}$ is the value at the central point of the static sigmoidal characteristic of arterial baroreceptors, and $f_{ac,0}$ is the central value in *Eq. A6*. $f_{es,0}$, $f_{es,\infty}$, k_{es}, $f_{ev,0}$, $f_{ev,\infty}$, and k_{ev} are constant parameters with the same value used previously (40). $f_{es,cc}$ and $f_{ev,cc}$ are offset terms added to reproduce the activation of the autonomic nervous system by motor central command during exercise. Both are set to 0 in resting conditions. Finally $G_{ab,j}$, $G_{ac,j}$ (j = p, v, h), $G_{ab,vag}$, and $G_{ac,vag}$ are constant gains.

The gains of arterial baroreceptor mechanism ($G_{ab,j}$, j = p, v, h and $G_{ab,vag}$) have been maintained at the same value used in the previous work. In contrast, all the parameters characterizing cardiopulmonary baroreceptors (f_{maxl}, k_l in *Eq. A6*, and the gains $G_{ac,j}$, j = p, v, h and $G_{ac,vag}$ in *Eqs. A9* and *A11*) have been set to simulate results of LBNP experiments in humans (4, 24). When performing these simulations, we assumed that venous compliance of the lower extremities (to which the LBNP is applied) is about one-tenth of the overall systemic venous compliance (i.e., ~10 ml/mmHg). This choice warrants a volume shift to the lower limbs by ~500 ml, when the LBNP is −50 mmHg (4). It is interesting to note that to reproduce the results of these experiments, we have to assume that the effect of cardiopulmonary baroreceptors on venous unstressed volumes is quite negligible (hence, the corresponding gains are set to 0, see Table 1).

Sensitivity Analysis

The sensitivity analysis on UC has been performed by individually modifying some of the key cardiovascular quantities (see Table 2). The alteration in the examined quantities has been produced in different ways depending on whether the quantity is a constant parameter in the model or is a parameter controlled by the sympathetic drive.

The constant parameters V_t (total blood volume), C_{sv}, C_{ev}, C_{mv}, and C_v (splanchnic and extrasplanchnic venous compliances, compliance of active muscle veins, and compliance of systemic thoracic veins), $V_{u,lv}$ (x-axis intercept of the left ventricle end-systolic pressure-volume curve) have been altered as follows: V_t from 5,019 to 5,600 ml; C_{sv} from 43.11 to 25 ml/mmHg; C_{ev} from 28.4 to 17 ml/mmHg; C_{mv} from 6.6 to 4 ml/mmHg; C_v from 33 to 20 ml/mmHg; $V_{u,lv}$ from 16.7 to −5 ml.

To simulate an alteration in the quantities $V_{u,sv}$, $V_{u,ev}$, and $V_{u,mv}$ (venous unstressed volume of splanchnic, extrasplanchnic, and active muscle circulation, respectively), $E_{max,lv}$ (slope of the left ventricular end-systolic pressure-volume curve), R_{sp}, R_{ep}, and R_{mp} (splanchnic, extrasplanchnic, and active muscle peripheral resistances, respectively), which are under sympathetic control, the corresponding static characteristic "parameter value vs. sympathetic activity" has been shifted to the left. Hence, we have

$$\theta = \begin{cases} \theta_0 + G_\theta \cdot \ln(f_{es,j} - f_{es,min} + 1 + B_\theta), & f_{es,j} \geq f_{es,min} \\ \theta_0, & f_{es,j} < f_{es,min} \end{cases} \quad j = p, v, h \tag{A12}$$

where θ denotes the generic controlled parameter (peripheral resistances, venous unstressed volumes, heart contractility, respectively). *Equation A12* represents the effector static characteristic used in the previous work (40), with the addition of an offset term B_θ. In particular, $f_{es,j}$ (j = p, v, h) is the frequency of spikes in the efferent sympathetic nerve to peripheral resistances, to veins, and to the heart, respectively, $f_{es,min}$ is the minimum sympathetic stimulation, G_θ are constant gain factors, and θ_0 is the parameter value in the absence of any sympathetic drive. To simulate a chronic alteration in the corresponding effector response, the offset term B_θ has been set equal to 10 spikes/s, otherwise it is kept equal to 0.

Simulations of Exercise Conditions

Several changes are introduced in the model to simulate exercise conditions. The first modification is that intramuscular pressure (P_{im}), which is extravascular pressure outside the active muscle veins, exhibits a periodical pattern. We assumed that at rest P_{im} is null, whereas during exercise it changes periodically according to the following equations

$$P_{im} = A \cdot \Psi(t) \tag{A13}$$

$$\Psi(t) = \begin{cases} \sin\left(\pi \cdot \frac{T_{im}}{T_c} \cdot \alpha\right), & 0 \leq \alpha \leq \frac{T_c}{T_{im}} \\ 0, & \frac{T_c}{T_{im}} \leq \alpha \leq 1 \end{cases} \tag{A14}$$

where A is the peak value of intramuscular pressure, which is the value of P_{im} at the instant of maximum contraction, and $\psi(t)$ is the activation function of skeletal muscle fibers [with $\psi(t) = 1$ at maximum contraction, $\psi(t) = 0$ at complete

relaxation]. T_{im} is the duration of the muscular contraction-relaxation cycle, and T_c is the overall duration of contraction (the part of T_{im} during which P_{im} is above 0). Finally, α is a dimensionless variable, ranging between 0 and 1, representing the fraction of the muscular contraction-relaxation cycle. The value $\alpha = 0$ conventionally corresponds to the beginning of contraction. An expression for $\alpha(t)$ may be obtained by introducing an additional state variable, $\zeta(t)$

$$\frac{d\zeta}{dt} = \frac{1}{T_{im}} \quad \text{with} \quad \alpha(t) = \text{frac}(\zeta) \qquad (A15)$$

where the function "fractional part" [frac( )] resets the variable $\alpha(t)$ to zero as soon as it reaches the value of +1.

Values assigned to the parameters A, T_{im}, and T_c (see Table 1) allow a good reproduction of intramuscular pressure temporal course measured in human volunteers (31).

The second modification is the frequency and depth of breathing increase. In particular, compared with rest, the respiratory period T_{resp} has been decreased during exercise, the inspiratory duty cycle T_i/T_{resp} has been increased, whereas the respiratory pause has been set equal to 0. Finally, to reproduce a deeper inspiration and an active expiration, intrathoracic pressure variation has been augmented by decreasing $P_{thor,min}$ and increasing $P_{thor,max}$. Values of intrathoracic pressure parameters during both mild and moderate exercise (see Table 1) have been given according to previous studies (11, 23, 37, 41).

The third modification is that sympathetic activity increases while the vagal one decreases. These modifications, which mimic the stimulus of motor impulses from the cerebral cortex to the cardiovascular control centers (the so-called "motor central command"), have been introduced by giving a positive value to the offset terms, $f_{es,cc}$ and $f_{ev,cc}$, in *Eqs. A8* and *A10*, respectively. Values assigned to these terms, at the two levels of exercise intensity, have been tuned to reproduce the changes in the main hemodynamic quantities observed in human volunteers (28) (Fig. 5).

Finally, the peripheral resistance of active muscle is reduced to simulate metabolic vasodilation. To this aim, we introduced a resistance R_d ($R_d = 1/G_d$) arranged in parallel, to empirically simulate the increase in muscle blood flow due to augmented metabolic need (see Figs. 1 and 2). Parameter R_d has been set at a very high level in resting conditions, so that it results negligible in the parallel arrangement, whereas at two exercise levels it has been tuned to reproduce the increase in systemic vascular conductance reported in Pawelczyk et al. (28).

REFERENCES

1. **Akagi T, Benson LN, Green M, Ash J, Gilday DL, Williams WG, and Freedom RM.** Ventricular performance before and after Fontan repair for univentricular atrioventricular connection: angiographic and radionuclide assessment. *J Am Coll Cardiol* 20: 920–926, 1992.
2. **Akagi T, Benson LN, Green M, De Souza M, Harder JR, Gilday DL, and Freedom RM.** Ventricular function during supine bicycle exercise in univentricular connection with absent right atrioventricular connection. *Am J Cardiol* 67: 1273–1278, 1991.
3. **Beneken JEW and De Wit B.** A physical approach to hemodynamic aspects of the human cardiovascular system. In: *Physical Bases of Circulatory Transport: Regulation and Exchange*, edited by Reeve EB and Guyton AC. Philadelphia, PA: Saunders, 1967, p. 1–45.
4. **Blomqvist CG and Stone HL.** Cardiovascular adjustments to gravitational stress. In: *Handbook of Physiology. The Cardiovascular System. Peripheral Circulation and Organ Blood Flow.* Bethesda, MD: Am Physiol Soc, 1983, sect. 2, vol. III, pt. 2, chapt. 28, p. 1025–1063.
5. **Coote JH.** Cardiovascular responses to exercise: central and reflex contributions. In: *Cardiovascular Regulation*, edited by Jordan D and Marshall J. London: Portland, 1995, p. 93–111.
6. **Fontan F and Baudet E.** Surgical repair of tricuspid atresia. *Thorax* 26: 240–248, 1971.
7. **Fontan F, Deville C, Quaegebeur J, Ottenkamp J, Sourdille N, Choussat A, and Brom GA.** Repair of tricuspid atresia in 100 patients. *J Thorac Cardiovasc Surg* 85: 647–660, 1983.
8. **Fredriksen PM, Therrien J, Veldtman G, Warsi MA, Liu P, Siu S, Williams WG, Granton J, and Webb G.** Lung function and aerobic capacity in adult patients following modified Fontan procedure. *Heart* 85: 295–299, 2001.
9. **Freyschuss U.** Cardiovascular adjustment of somatomotor activation. *Acta Physiol Scan* 342, *Suppl* 1: 1–63, 1970.
10. **Gale AW, Danielsson GK, McGoon DC, and Mair DD.** Modified Fontan operation for univentricular heart and complicated congenital lesions. *J Thorac Cardiovasc Surg* 78: 831–838, 1979.
11. **Gardner WN and Meah MS.** Respiration during exercise in conscious laringectomized humans. *J Appl Physiol* 66: 2071–2078, 1989.
12. **Humes RA, Porter CJ, Mair DD, Rice MJ, Offord KP, Puga FJ, Schaff HV, and Danielson GK.** Intermediate follow-up and predicted survival after the modified Fontan procedure for tricuspid atresia and double-inlet ventricle. *Circulation* 76, *Suppl* III: 67–71, 1987.
13. **Innes JA, De Cort SC, Kox W, and Guz A.** Within-breath modulation of left ventricular function during normal breathing and positive-pressure ventilation in man. *J Physiol (Lond)* 460: 487–502, 1993.
14. **Kaulitz R, Ziemer G, Luhmer I, and Kallfelz HC.** Modified Fontan operation in functionally univentricular hearts: preoperative risk factors and intermediate results. *J Thorac Cardiovasc Surg* 112: 658–664, 1996.
15. **Kelley JR, Mack GW, and Fahey JT.** Diminished venous vascular capacitance in patients with univentricular hearts after the Fontan operation. *Am J Cardiol* 76: 158–163, 1995.
16. **Kresh JY, Brockman SK, and Noordergraaf A.** Theoretical and experimental analysis of right ventricular bypass and univentricular circulatory support. *IEEE Trans Biomed Eng* 37: 121–127, 1990.
17. **Lash JM and Shoukas AA.** Pressure dependence of baroreceptor-mediated vasoconstriction in rat skeletal muscle. *J Appl Physiol* 70: 2551–2558, 1991.
18. **Leonard B, Mitchell JH, Mizuno M, Rube N, Saltin B, and Secher NH.** Partial neuromuscular blockade and cardiovascular responses to static exercise in men. *J Physiol (Lond)* 359: 365–379, 1985.
19. **Levick JR.** *An Introduction to Cardiovascular Physiology*. Oxford, UK: Butterworth-Heinemann, 1991.
20. **Levy MN and Zieske H.** Autonomic control of cardiac pacemaker activity and atrioventricular transmission. *J Appl Physiol* 27: 465–470, 1969.
21. **Macé L, Dervanian P, Bourriez A, Mazmanian GM, Lambert V, Losay J, and Neveux J.** Changes in venous return parameters associated with univentricular Fontan circulations. *Am J Physiol Heart Circ Physiol* 279: H2335–H2343, 2000.
22. **Mavroudis C, Backer CL, Deal BJ, and Johnsrude CL.** Fontan conversion to cavopulmonary connection and arrhytmia circuit cryoablation. *J Thorac Cardiovasc Surg* 115: 547–556, 1998.
23. **Milic-Emili J and Zinn WA.** Relationship between neuromuscular resoiratory drive and ventilatory output. In: *Handbook of Physiology. The Respiratory System. Mechanics of Breathing.* Bethesda, MD: Am Physiol Soc, 1986, sect. 3, vol III, pt. 2, chapt. 35, p. 631–646.
24. **Mohanty PK, Thames MD, Arrowood JA, Sowers JR, McNamara C, and Szentpetery S.** Impairment of cardiopulmonary baroreflex after cardiac transplantation in humans. *Circulation* 75: 914–921, 1987.
25. **Moreno AH, Katz AI, and Gold LD.** An integrated approach to the study of the venous system with steps toward a detailed

model of the dynamics of venous return to the right heart. *IEEE Trans Biomed Eng* 16: 308–324, 1969.
26. **Nokagi M, Senzaki H, Masutani S, Kobayashi J, Kobayashi T, Sasaki N, Asano H, Kyo S, and Yokote Y.** Ventricular energetics in Fontan circulation: evaluation with a theoretical model. *Pediatr Int* 42: 651–657, 2000.
27. **Norwood WI, Kirklin JK, and Sanders SP.** Hypoplastic left heart syndrome; experience with palliative surgery. *Am J Cardiol* 45: 87–91, 1980.
28. **Pawelczyk JA, Hanel B, Pawelczyk RA, Warberg J, and Secher NH.** Leg vasoconstriction during dynamical exercise with reduced cardiac output. *J Appl Physiol* 73: 1838–1846, 1992.
29. **Pedley TJ.** *The Fluid Mechanics of Large Blood Vessels*. Cambridge, UK: Cambridge University Press, 1980.
30. **Pennati G, Migliavacca F, Dubini G, Pietrabissa R, and de Leval MR.** A mathematical model of circulation in the presence of the bidirectional cavopulmonary anastomosis in children with a univentricular heart. *Med Eng Phys* 19: 223–234, 1997.
31. **Rådegran G and Saltin B.** Muscle blood flow at onset of dynamic exercise in humans. *Am J Physiol Heart Circ Physiol* 274: H314–H322, 1998.
32. **Rothe CF.** Reflex control of veins and vascular capacitance. *Physiol Rev* 63: 1281–1342, 1983.
33. **Rowell LB.** *Human Cardiovascular Control*. New York: Oxford University Press, 1993.
34. **Rydberg A, Teien DE, and Krus P.** Computer simulation of circulation in patient with total cavo-pulmonary connection: inter-relationship of cardiac and vascular pressure, flow, resistance and capacitance. *Med Biol Eng Comput* 35: 722–728, 1997.
35. **Sanders SP, Wright GB, Keane JF, Norwood WI, and Castaneda AR.** Clinical and hemodynamic results of the Fontan operation for tricuspid atresia. *Am J Cardiol* 49: 1733–1740, 1982.
36. **Shachar GB, Fuhrman BP, Wang Y, Lucas RV, and Lock JE.** Rest and exercise hemodynamics after the Fontan procedure. *Circulation* 65: 1043–1048, 1982.
37. **Sheldahl LM, Tristani FE, Clifford PS, Hughes CV, Sobocinski KA, and Morris RD.** Effect of head-out water immersion on cardiorespiratory response to dynamical exercise. *J Am Coll Cardiol* 10: 1254–1258, 1987.
38. **Shoukas AA and Sagawa K.** Control of total systemic vascular capacity by the carotid sinus baroreceptor reflex. *Circ Res* 33: 22–32, 1973.
39. **Troutman WB, Barstow TJ, Galindo AJ, and Cooper DM.** Abnormal dynamic cardiorespiratory responses to exercise in pediatric patients after Fontan procedure. *J Am Coll Cardiol* 31: 668–673, 1998.
40. **Ursino M.** Interaction between carotid baroregulation and the pulsating heart: a mathematical model. *Am J Physiol Heart Circ Physiol* 275: H1733–H1747, 1998.
41. **Whipp BJ and Pardy RL.** Breathing during exercise. In: *Handbook of Physiology. The Respiratory System. Mechanics of Breathing.* Bethesda, MD: Am Physiol Soc, 1986, sect. 3, vol. III, pt. 2, chapt. 34, p. 605–629.
42. **Zellers TM, Driscoll DJ, Mottram CD, Puga FJ, Hartzell VS, and Danielson GK.** Exercise tolerance and cardiorespiratory response to exercise before and after the Fontan operation. *Mayo Clin Proc* 64: 1489–1497, 1989.